

Impact ionization fronts in Si diodes: Numerical evidence of superfast propagation due to nonlocalized preionization

Pavel Rodin^{1*}, Andrey Minarsky² and Igor Grekhov¹

¹ Ioffe Physicotechnical Institute, Politechnicheskaya 26, 194021, St.-Petersburg, Russia,

² Physico-Technical High School of Russian Academy of Science, Khlopina 8-3, 194021, St.-Petersburg, Russia

(Dated: January 24, 2010)

We present numerical evidence of a novel propagation mode for superfast impact ionization fronts in high-voltage Si p^+-n-n^+ structures. In nonlinear dynamics terms, this mode corresponds to a pulled front propagating into an unstable state in the regime of nonlocalized initial conditions. Before the front starts to travel, field-enhanced emission of electrons from deep-level impurities preionizes initially depleted n base creating spatially nonuniform free carriers profile. Impact ionization takes place in the whole high-field region. We find two ionizing fronts that propagate in opposite directions with velocities up to 10 times higher than the saturated drift velocity.

PACS numbers: 72.20.Ht, 85.30.-z,

Superfast impact ionization fronts travel with velocity v_f higher than the saturated drift velocity v_s . Excitation of such fronts is the fastest non-optical method to modulate conductivity of a high-voltage semiconductor structure.²⁻⁴ This method has important pulse-power application.⁵⁻⁷ Recently, we proposed a novel mode of superfast front propagation in semiconductor structures: a pulled front propagating into unstable state in the regime of nonlocalized initial conditions.⁸ This mode is expected to appear in p^+-n-n^+ structures with a relatively low n base doping level. The propagation mechanism is qualitatively different from that for the well-known TRAPATT-like propagation mode,¹⁰⁻¹² widely considered as a most feasible mechanism of the superfast switching of high-voltage pulse-power devices.² For the impact ionization front the term “nonlocalized initial conditions”¹³ means a small free carriers concentration that decreases in the direction of front propagation. It has been suggested⁸ that such preionization of the initially depleted n base may be created by field-enhanced electron emission from deep-level centers.⁹ Numerical simulations presented in the Letter confirms this suggestion and provide the first evidence of superfast front propagation due to nonlocalized preionization in realistic Si p^+-n-n^+ structures used in pulse-power applications.

Process-induced (PI) deep-level centers in Si are double-charged donors with ionization energies 0.28 eV (II level) and 0.54 eV (M level)^{14,15} Originally thought

of as recombination centers,¹⁴ PI centers turned out to be deep electron traps.¹⁵ As they do not influence the life-time of nonequilibrium carriers (the most carefully controlled parameter of the commercial material), their presence in high-purity Si is “hidden”.¹⁵ In high voltage structures used in power applications PI centers appear in concentration $N_{PI} = 10^{11} \dots 10^{13} \text{ cm}^{-3}$ (Ref. 15). Field-enhanced ionization of PI centers is a potential mechanism of deterministic low-jitter triggering of the ionizing front in high-voltage structures.⁹ In the simplest case of low temperatures ($T < 200 \text{ K}$) the emission rate depends on the electrical field F as (Ref. 9)

$$\epsilon(F) = \frac{F}{\sqrt{8mE_0}} \exp\left(-\frac{F_0}{F}\right) \exp\left(2\sqrt{\frac{E_B}{E_0}} \ln \frac{6F_0}{F}\right), \quad (1)$$

where $F_0 \equiv 4\sqrt{2mE_0^3}/3q\hbar$, $E_0 = 0.28 \text{ eV}$ is the binding energy (U level), E_B is Bohr energy in semiconductor, m is the effective electron mass and q is the elementary charge. Field-enhanced ionization of PI centers has a characteristic threshold $F_{th}^{PI} \approx 3 \cdot 10^5 \text{ V/cm}$ (Ref. 9) that exceeds the threshold of band-to-band impact ionization $F_{th}^{imp} \approx 2 \cdot 10^5 \text{ V/cm}$. It is important that $F_{th}^{PI} > F_{th}^{imp}$ because electrical field in the n base should be increased above F_{th}^{imp} before impact ionization starts.⁹

Superfast triggering occurs when a sharp voltage ramp is applied to reversely biased Si p^+-n-n^+ structure connected to the voltage source $V(t)$ in series with load resistance R (Fig. 1). The applied voltage is modelled as $V(t) = V_0 + A \cdot t$, where the initial voltage V_0 is chosen so that the n base is fully depleted at $t = 0$. We assume that p^+-n and $n-n^+$ junctions are sharp and restrict modelling to the n base. To describe the dynamics of electron and hole concentrations $n(z, t)$, $p(z, t)$ and electrical field $F(z, t)$, we use the standard one-dimensional drift-diffusion model together with the Poisson equation and the Kirchoff equation for the external circuit. The generation term includes the cut-off that eliminates unphysical multiplication at low concentrations $n, p < n_{cut}$.¹⁹ We refer to Ref. 19 for the details of the model and of the numerical method used. The generation term addi-

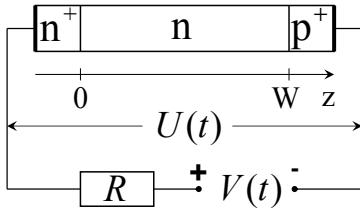


FIG. 1: Sketch of the reversely biased p^+-n-n^+ -structure operated in the external circuit.

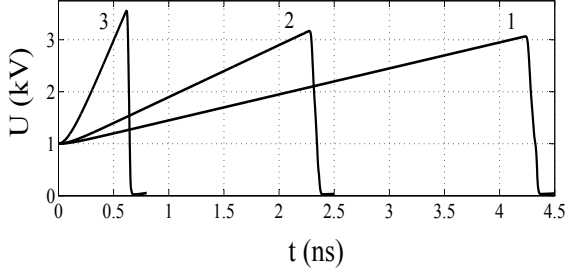


FIG. 2: Voltage $U(t)$ during the switching process for different voltage ramps $A = 0.5, 1, 5$ kV/ns (curves 1, 2 and 3, respectively).

tionally incorporates field-enhanced emission of free electrons from PI centers with a rate given by Eq. (1). We use the following set of structure and circuit parameters: the n base length $W = 100 \mu\text{m}$, dopant concentration $N_d = 10^{13} \text{ cm}^{-3}$, $N_{PI} = 10^{12} \text{ cm}^{-3}$, cross-section area $S = 0.02 \text{ cm}^2$, load resistance $R = 50 \text{ Ohm}$, initial bias $V_0 = 1 \text{ kV}$. The respective stationary breakdown voltage is about 1.2 kV. We choose $n_{\text{cut}} = 10^9 \text{ cm}^{-3}$, as in Refs. 19, 20.

In Fig. 2 we show the voltage $U(t)$ over the diode during switching process. At the first stage $U(t)$ nearly follows the applied voltage $V(t)$. Then, $U(t)$ sharply drops and the current flowing through the diode increases. The triggering time is close to 100 ps and decreases with increase of the voltage ramp A . This is 10 times faster than the drift time $W/v_s \approx 1 \text{ ns}$. Such superfast switching has been observed in the whole range of actual voltage ramps 0.5...10 kV/ns. Although the transient $U(t)$ looks similar to the earlier numerical results for TRAPATT-like^{6,16–19} or tunneling-assisted^{20,21} impact ionization fronts, the inner dynamics turns out to be qualitatively different.

In Fig. 3 we show the inner dynamics for $A = 1 \text{ kV/ns}$. Due to the higher electrical field, the emission of electrons from PI centers is most efficient near p^+-n junction. Free electrons drift to the left and multiply by the band-to-band impact ionization. Due to this drift, the maximum of the concentration profile is shifted from the p^+-n junction into the n base [Fig. 3(a)]. Screening begins when concentrations n and p overcome N_d . Eventually, the avalanche multiplication creates the initial plasma layer that fully screens the applied electrical field [Fig. 3(a), curve 3]. Afterwards, the plasma layer expands due to propagation of two ionizing fronts travelling in opposite directions [Fig. 3(b)].

The left and the right (negative and positive) fronts travel with velocities $v_f^- \approx 10 v_s$ and $v_f^+ \approx 3 v_s$, respectively. Both fronts propagate into the areas where the electrical field F_m is nearly constant in space and varies in the interval from $3 \cdot 10^5$ to $4 \cdot 10^5 \text{ V/cm}$, nearly 2 times larger than $F_{\text{th}}^{\text{imp}}$. The small amount of free carriers is present everywhere (Fig. 4). Hence avalanche multiplication also goes on all over the high-field region. These con-

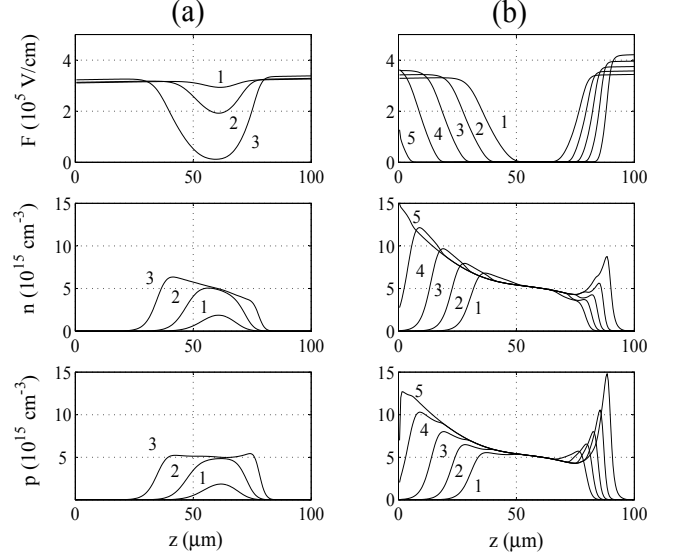


FIG. 3: The spatial profiles of the electrical field $F(z, t)$ and electron and hole concentrations $n(z, t)$ and $p(z, t)$ in the n -base at different times: (a) increase of the free carrier concentration due to the field-enhanced ionization of deep-level impurities and subsequent avalanche multiplication at times $t = 2.285, 2.295, 2.31 \text{ ns}$ (curves 1, 2, and 3, respectively); (b) propagation of impact ionization fronts at $t = 2.315, 2.325, 2.335, 2.345, 2.355 \text{ ns}$ (curves 1, 2, 3, 4, and 5, respectively). Numerical parameters as in Fig. 2 for $A = 1 \text{ kV/ns}$.

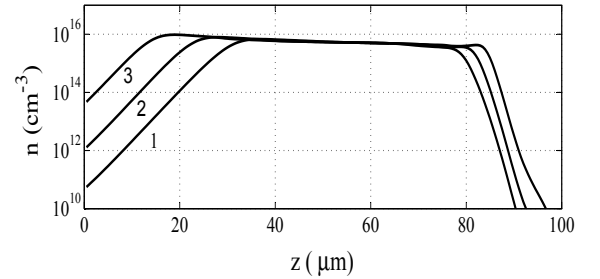


FIG. 4: The spatial profile of electron concentrations $n(z, t)$ in the propagating front at times $t = 2.315, 2.325, 2.335 \text{ ns}$ (curves 1, 2, and 3, respectively,) in logarithmic scale. Numerical parameters as in Fig. 3.

ditions are favorable for quasiuniform breakdown. The reason why the front-like solution nevertheless occurs is the nonuniform profile of preionization: the concentration of free carriers in the high-field region decreases in the direction of front propagation. This decay happens to be nearly exponential $n, p \sim \exp(\pm \lambda z)$ with characteristic exponents $\lambda^- \approx 4 \cdot 10^3 \text{ cm}^{-1}$ and $\lambda^+ \approx 1.3 \cdot 10^4 \text{ cm}^{-1}$ for negative and positive fronts, respectively (Fig. 4). In nonlinear dynamics, such fronts are known as pulled fronts propagating into unstable state in the regime of

nonlocalized initial conditions.¹³

Let us compare the numerical results with analytical predictions for front velocity and plasma concentration made in Ref. 8 for the simplified model where electrons and holes have the same impact ionization coefficients $\alpha(F) = \alpha_n(F) = \alpha_p(F)$ and $N_d = 0$. For sufficiently small exponent λ , the front velocity is given by

$$v_f/v_s \approx 2\alpha_m/\lambda, \quad (2)$$

where $\alpha_m \equiv \alpha(F_m)$ is the impact ionization coefficient in the high field region the front propagates to. In Si in strong electrical fields impact ionization by holes is much weaker than by electrons. Therefore $2\alpha_m$ shall be replaced by $\alpha_m \equiv \alpha_n(F_m)$ in the nominator of Eq. (2). The numerical value is $\alpha_m \approx 3.2 \cdot 10^4 \text{ cm}^{-1}$ for $F_m = 3.5 \cdot 10^5 \text{ V/cm}$. Eq. (2) is applicable if $\lambda \ll \lambda^*$, where λ^* corresponds to so called marginally stable front¹³ and is explicitly determined by α_m , diffusion coefficient D and v_s (see Ref. 8). Simple calculation shows that $\lambda^* \approx 2 \cdot 10^5 \text{ cm}^{-3}$. Hence, the condition $\lambda^\pm \ll \lambda^*$ is met for the case under consideration, and we obtain analytical estimates $v_f^- \approx \alpha_m/\lambda^- \approx 8v_s$ and $v_f^+ \approx \alpha_m/\lambda^+ \approx 2.5v_s$ for the negative and positive fronts shown in Figs. 3,4, respectively, in good agreement with numerical results.

For the symmetrical model, the plasma concentration $\sigma \equiv n + p$ behind the front is given by $\sigma_{pl} = (2\varepsilon\varepsilon_0\alpha_0 F_0/q) \int_0^{F_m/F_0} \exp(-1/x)dx$, where the ionization coefficient is approximated as $\alpha(F) = \alpha_0 \exp(-F_0/F)$ (Ref. 8). Removing again the factor of 2 and taking the numerical values $\alpha_0 = 7.4 \cdot 10^5 \text{ cm}$, $F_0 = 1.1 \cdot 10^6 \text{ V/cm}$

for electrons in Si, we get $\sigma_{pl} \approx 10^{16} \text{ cm}^{-3}$ for the actual electrical field $F_m = 3.5 \cdot 10^5 \text{ V/cm}$, in good agreement with numerical results.

The velocity of the convential TRAPATT-like front is determined by the size of impact ionization zone.^{10–12} In contrast, the velocity of the pulled front in the regime of nonlocalized initial conditions is determined by the slope of the preionization profile, while the size of impact ionization zone coincides with the total size of the high-field region. Consequently, the pulled fronts shall be expected in structures with moderate doping N_d where the condition $F > F_{th}^{imp}$ is met all over the high-field region. However, a certain level of the n base doping N_d is crucial because it leads to the slope of the electrical field in the depleted n base. Due to this slope the field-enhanced ionization of PI centers is spatially nonuniform and creates decaying profile of preionization. In particular, in $p-i-n$ structures nonlocalized initial conditons for the pulled front propagation cannot be created by deep-level impurities. For large N_d the convential TRAPATT-like mode^{10–12} occurs, but the cross-over to the pulled mode is possible at the last stage of front propagation when the condition $F > F_{th}^{imp}$ is met everywhere.

We are indebted to W. Hundsdorfer who has developed numerical tools used in the simulations. This work was supported by Russian Academy of Science in the framework of the project “Power semiconductor electronics and pulse technology”. P. Rodin is grateful to A. Alekseev for hospitality at the University of Geneva and acknowledges the support from the Swiss National Science Foundation.

-
- * Electronic address: rodin@mail.ioffe.ru
- ² M. Levinshtein, J. Kostamovaara, S. Vainshtein, *Breakdown Phenomena in Semiconductors and Semiconductor Devices* (Word Scientific, 2005).
 - ³ I.V. Grekhov and A.F. Kardo-Sysoev, *Sov. Tech. Phys. Lett.* **5**, 395 (1979).
 - ⁴ Zh.I. Alferov, I.V. Grekhov, V.M. Efanov, A.F. Kardo-Sysoev, V.I. Korol'kov, and M.N. Stepanova *Sov. Tech. Phys. Lett.* **13**, 454 (1987).
 - ⁵ I.V. Grekhov, *Solid-State Electron.* **32**, 923 (1989).
 - ⁶ R.J. Focia, E. Schamiloghu, C.B. Fledermann, F.J. Agee and J. Gaudet, *IEEE Trans. Plasma Sci.* **25**, 138 (1997).
 - ⁷ A.F. Kardo-Susoev, *New Power Semiconductor Devices for Generation of Nanosecond Pulses*, in *Ultra-Wideband Radar Technology*, edited by James D. Taylor, CRC Press, Boca Raton, London, New York, Washington, 2001, pp.205-209.
 - ⁸ P. Rodin, A. Minarsky, I. Grekhov, *Appl. Phys. Lett.* **93**, 013503 (2008).
 - ⁹ P. Rodin and I. Grekhov, *Appl. Phys. Lett.* **86**, 243504 (2005); P. Rodin, A. Rodina, and I. Grekhov, *J. Appl. Phys.* **98**, 094506 (2005).
 - ¹⁰ B.C. Deloach and D.L. Scharfetter, *IEEE Trans. Electron Devices* **ED-20**, 9 (1970).
 - ¹¹ A.S. Kyuregyan, *Semiconductors* **41**, 737 (2007).
 - ¹² P. Rodin, U. Ebert, A. Minarsky and I. Grekhov, *J. Appl. Phys.* **102**, 034508 (2007).
 - ¹³ W. van Saarloos, *Physics Reports* **386**, 29 (2003)
 - ¹⁴ L.D. Yau and C.T. Sah, *Solid-State Electronics* **17**, 193(1974); *J. Apl. Phys.* **46**, 1767 (1975).
 - ¹⁵ E.V. Astrova, V.B. Voronkov, V.A. Kozlov and A.A. Lebedev, *Semicond. Sci. Technol.* **13**, 488-495 (1998).
 - ¹⁶ Yu.D. Bilenko, M.E. Levinstein, M.V. Popova and V.S. Yuferev, *Sov. Phys. Semicond.* **17**, 1156 (1983).
 - ¹⁷ A.F. Kardo-Susoev and M.V. Popova, *Sov. Phys. Semicond.* **30**, 431 (1996).
 - ¹⁸ H. Jalali, R. Joshi, and J. Gaudet, *IEEE Trans. Electron Devices* **45**, 1761-1768(1998).
 - ¹⁹ P. Rodin, U. Ebert, W. Hundsdorfer, and I. Grekhov, *J. Appl. Phys.* **92**, 1971 (2002).
 - ²⁰ P. Rodin, U. Ebert, W. Hundsdorfer, and I. Grekhov, *J. Appl. Phys.* **92**, 958 (2002).
 - ²¹ S.K. Lyubutin, S.N. Rukin, B.G. Slovikovsky, S.N. Tsyranov, *Tech. Phys. Lett.* **31**, 196 (2005).